

Multi-trait analysis of genome-wide association summary statistics using MTAG

Patrick Turley^{1,2*}, Raymond K. Walters^{1,2}, Omeed Maghziyan³, Aysu Okbay⁴, James J. Lee⁵, Mark Alan Fontana⁶, Tuan Anh Nguyen-Viet⁷, Robbee Wedow^{8,9,10}, Meghan Zacher¹¹, Nicholas A. Furlotte¹², 23andMe Research Team¹³, Social Science Genetic Association Consortium¹⁴, Patrik Magnusson¹⁵, Sven Oskarsson¹⁶, Magnus Johannesson¹⁷, Peter M. Visscher^{18,19}, David Laibson^{3,20}, David Cesarini^{20,21,22*}, Benjamin M. Neale^{1,2*}, Daniel J. Benjamin^{7,20,23*}

We introduce multi-trait analysis of GWAS (MTAG), a method for joint analysis of summary statistics from genome-wide association studies (GWAS) of different traits, possibly from overlapping samples. We apply MTAG to summary statistics for depressive symptoms ($N_{\text{eff}} = 354,862$), neuroticism ($N = 168,105$), and subjective well-being ($N = 388,538$). As compared to the 32, 9, and 13 genome-wide significant loci identified in the single-trait GWAS (most of which are themselves novel), MTAG increases the number of associated loci to 64, 37, and 49, respectively. Moreover, association statistics from MTAG yield more informative bioinformatics analyses and increase the variance explained by polygenic scores by approximately 25%, matching theoretical expectations.

The standard approach in genetic association studies is to analyze a single trait. Such studies do not exploit information contained in summary statistics from GWAS of related traits. In this report, we develop a method, multi-trait analysis of GWAS (MTAG), that enables joint analysis of multiple traits, thus boosting statistical power to detect genetic associations for each trait analyzed.

In comparison to the many existing multi-trait methods^{1–5}, MTAG has a unique combination of four features that make it potentially useful in many settings. First, it can be applied to GWAS summary statistics (without access to individual-level data) from an arbitrary number of traits. Second, the summary statistics need not come from independent discovery samples: MTAG uses bivariate linkage disequilibrium (LD) score regression⁶ to account for (possibly unknown) sample overlap between the GWAS results for different traits. Third, MTAG generates trait-specific effect estimates for each SNP. Finally, even when applied to many traits, MTAG is computationally quick because every step has a closed-form solution.

The MTAG estimator is a generalization of inverse-variance-weighted meta-analysis that takes summary statistics from single-trait GWAS and outputs trait-specific association statistics. The resulting P values can be used like P values from a single-trait

GWAS, for example, to prioritize SNPs for subsequent analyses such as biological annotation or to construct polygenic scores.

The key assumption of MTAG is that all SNPs share the same variance–covariance matrix of effect sizes across traits. This assumption is strong and is violated in many circumstances, most intuitively in scenarios where some SNPs influence only a subset of the traits. Even if this assumption is not satisfied, however, we show analytically that MTAG is a consistent estimator and that its effect estimates always have a lower genome-wide mean-squared error (MSE) than the corresponding single-trait GWAS estimates. Hence, polygenic scores constructed from MTAG results are expected to outperform GWAS-based predictors very generally.

The main potential problem arises for SNPs that are truly null for one trait but non-null for another trait. For such SNPs, MTAG's effect size estimates for the first trait are biased away from zero, leading to an increased rate of false positives (and an inflated type I error rate). We derive an analytic formula for the resulting false discovery rate (FDR), given any specified mixture-normal distribution of effect sizes (including multivariate spike-and-slab distributions), and we illustrate how the formula can be used to probe the credibility of MTAG-identified loci.

¹Broad Institute, Cambridge, MA, USA. ²Analytic and Translational Genetics Unit, Massachusetts General Hospital, Cambridge, MA, USA.

³Department of Economics, Harvard University, Cambridge, MA, USA. ⁴Department of Complex Trait Genetics, Vrije Universiteit Amsterdam, Amsterdam, The Netherlands. ⁵Department of Psychology, University of Minnesota, Minneapolis, MN, USA. ⁶Hospital for Special Surgery, New York, NY, USA.

⁷Center for Economic and Social Research, University of Southern California, Los Angeles, CA, USA. ⁸Institute for Behavioral Genetics, University of Colorado Boulder, Boulder, CO, USA. ⁹Institute of Behavioral Science, University of Colorado Boulder, Boulder, CO, USA. ¹⁰Department of Sociology, University of Colorado Boulder, Boulder, CO, USA. ¹¹Department of Sociology, Harvard University, Cambridge, MA, USA. ¹²23andMe, Inc., Mountain View, CA, USA. ¹³A list of members and affiliations appears at the end of the paper. ¹⁴A list of members and affiliations appears in the Supplementary Note.

¹⁵Institutionen för Medicinsk Epidemiologi och Biostatistik, Karolinska Institutet, Stockholm, Sweden. ¹⁶Department of Government, Uppsala Universitet, Uppsala, Sweden. ¹⁷Department of Economics, Stockholm School of Economics, Stockholm, Sweden. ¹⁸Institute for Molecular Bioscience, University of Queensland, Brisbane, Queensland, Australia. ¹⁹Queensland Brain Institute, University of Queensland, Brisbane, Queensland, Australia. ²⁰National Bureau of Economic Research, Cambridge, MA, USA. ²¹Department of Economics and Center for Experimental Social Science, New York University, New York, NY, USA. ²²Institutet för Näringslivsforskning, Stockholm, Sweden. ²³Department of Economics, University of Southern California, Los Angeles, CA, USA.

Patrick Turley, David Cesarini, Benjamin M. Neale and Daniel J. Benjamin contributed equally to this work. *e-mail: paturley@broadinstitute.org; dac12@nyu.edu; bneale@broadinstitute.org; daniel.benjamin@gmail.com

To demonstrate the utility of MTAG empirically, we analyze three traits: depressive symptoms (DEP; $N_{\text{eff}}=354,862$), neuroticism (NEUR; $N=168,105$), and subjective well-being (SWB; $N=388,538$). Prior GWAS of each of these traits have identified only a handful of loci^{7–11}. Because of the high genetic correlations between the three traits—in our data, roughly 0.7 in absolute value for each pair—some papers have conducted cross-trait analyses to replicate findings for one of the traits¹¹ or joint meta-analysis to identify new loci⁵. We applied MTAG to these traits because we expected that the gains in power would be substantial, the violations of MTAG's assumptions would be limited, and the substantive results would be of interest.

Finally, we compare MTAG to the three existing multi-trait methods we are aware of that can be applied to GWAS summary statistics from an arbitrary number of traits with unknown sample overlap^{12,13}. We find that MTAG has greater power across a wide range of simulation scenarios and in two separate applications to real data.

Results

Overview of MTAG. The key idea underlying MTAG is that, when GWAS estimates from different traits are correlated, the effect estimates for each trait can be improved by appropriately incorporating information contained in the GWAS estimates for the other traits.

Correlation between GWAS estimates can arise for two reasons. First, the traits may be genetically correlated, in which case the true effects of the SNPs are correlated across traits. Second, the estimation error of the SNPs' effects may be correlated across traits. Such correlation will occur if (i) the phenotypic correlations are nonzero and there is sample overlap across traits or (ii) biases in the SNP effect estimates (for example, population stratification or cryptic relatedness) have correlated effects across traits. MTAG boosts statistical power by incorporating information about these two sources of correlation.

MTAG framework. In the framework that follows, all traits and genotypes are standardized to have mean zero and variance one. For SNP j , we denote the vector of marginal (i.e., not controlling for other SNPs), true effects on each of the T traits by β_j . We treat these true effects as random effects with $E(\beta_j) = \mathbf{0}$ and $\text{var}(\beta_j) = \mathbf{\Omega}$. If the true effects are correlated across traits, then the off-diagonal elements of $\mathbf{\Omega}$ are nonzero. MTAG's key assumption is that $\mathbf{\Omega}$ is homogeneous across SNPs, i.e., that it does not depend on j .

We denote the vector of GWAS estimates of the effects for SNP j on the traits by $\hat{\beta}_j$. We assume that the GWAS estimates are unbiased, $E(\hat{\beta}_j | \beta_j) = \beta_j$, and we denote the variance–covariance matrix of their estimation error by $\text{var}(\hat{\beta}_j | \beta_j) = \mathbf{\Sigma}_j$. The off-diagonal elements of $\mathbf{\Sigma}_j$ are nonzero whenever the estimation errors are correlated.

MTAG is an efficient generalized method of moments (GMM) estimator based on the moment condition

$$E\left(\hat{\beta}_j - \frac{\omega_t}{\omega_{tt}} \beta_{j,t}\right) = \mathbf{0}$$

where ω_t is a vector equal to the t th column of $\mathbf{\Omega}$ and ω_{tt} is a scalar equal to the t th diagonal element of $\mathbf{\Omega}$. This equality is a necessary condition derived from the best linear prediction of the vector of GWAS estimates, $\hat{\beta}_j$, from the SNP's true effect on a single trait, $\beta_{j,t}$. The MTAG estimator is a weighted sum of the GWAS estimates

$$\hat{\beta}_{\text{MTAG},j,t} = \frac{\frac{\omega_t}{\omega_{tt}} \left(\mathbf{\Omega} - \frac{\omega_t \omega_t'}{\omega_{tt}} + \mathbf{\Sigma}_j \right)^{-1}}{\frac{\omega_t}{\omega_{tt}} \left(\mathbf{\Omega} - \frac{\omega_t \omega_t'}{\omega_{tt}} + \mathbf{\Sigma}_j \right)^{-1} \frac{\omega_t}{\omega_{tt}}} \hat{\beta}_j \quad (1)$$

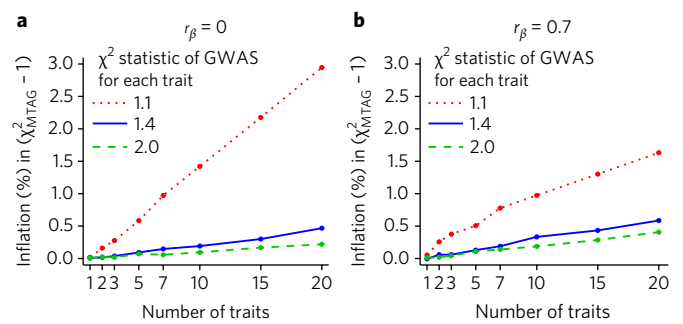


Fig. 1 | Bias in standard errors from ignoring sampling variation in $\hat{\Sigma}$ and $\hat{\Omega}$. **a, b.** The y axis shows the percentage increase in $(\chi^2 - 1)$ of the MTAG test statistics from using estimated values of $\mathbf{\Sigma}$ and $\mathbf{\Omega}$ rather than the true values. Each line corresponds to results from applying MTAG to identically powered single-trait GWAS of T traits. For every pair of traits, the correlation in true effect sizes is $r_\beta = 0$ (**a**) or $r_\beta = 0.7$ (**b**). Complete results for the full set of simulation scenarios can be found in the Supplementary Note.

It is a consistent and asymptotically normal estimator for $\beta_{j,t}$ (Supplementary Note).

There are several useful special cases of MTAG (Methods). When all estimates are for the same trait (implying $\frac{\omega_t \omega_t'}{\omega_{tt}} = \mathbf{\Omega}$ and $\frac{\omega_t}{\omega_{tt}} = 1$), equation (1) simplifies to

$$\hat{\beta}_{\text{MTAG},j,t} = \frac{\mathbf{1}' \mathbf{\Sigma}_j^{-1}}{\mathbf{1}' \mathbf{\Sigma}_j^{-1} \mathbf{1}} \hat{\beta}_j$$

When the GWAS estimates are obtained from non-overlapping samples (i.e., $\mathbf{\Sigma}_j$ is diagonal), this formula specializes to the well-known formula for inverse-variance-weighted meta-analysis. When the genetic correlations across all traits are zero and there is no sample overlap (i.e., when both $\mathbf{\Omega}$ and $\mathbf{\Sigma}_j$ are diagonal), the MTAG estimates are identical to the GWAS estimates. This equivalence is intuitive, as it corresponds exactly to the case of no correlation between the GWAS estimates that can be leveraged.

To make equation (1) operational, we use the consistent estimates of $\mathbf{\Sigma}_j$ and $\mathbf{\Omega}$ described next (Supplementary Note).

Estimation of $\mathbf{\Sigma}_j$. In standard meta-analysis, the diagonal elements of $\hat{\mathbf{\Sigma}}_j$ would be constructed using the squared standard errors from the GWAS results and the off-diagonal elements of $\hat{\mathbf{\Sigma}}_j$ would be set to zero. In MTAG, however, we want to allow the estimation error to include bias (in addition to sampling variation) and to be correlated across the GWAS estimates.

Therefore, MTAG proceeds by running LD score regressions¹⁴ on the GWAS results and using the estimated intercepts to construct the diagonal elements of $\hat{\mathbf{\Sigma}}_j$. Next, bivariate LD score regressions⁶ are run using each pair of GWAS results, and the estimated intercepts are used to construct the off-diagonal elements of $\hat{\mathbf{\Sigma}}_j$. Under the assumptions of LD score regression (including that the LD reference sample and GWAS samples all be drawn from the same population), the resulting matrix $\hat{\mathbf{\Sigma}}_j$ captures all relevant sources of estimation error, including not only sampling variation but also population stratification, unknown sample overlap, and cryptic relatedness. Because the LD-score-intercept adjustment is already built into MTAG estimates, MTAG-generated association results do not require further adjustment for these biases.

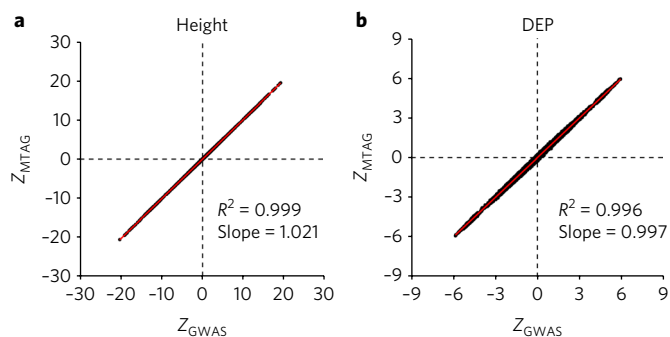


Fig. 2 | Evaluation of MTAG's standard error when there is sample overlap. The x axis shows a SNP's z statistic from a baseline GWAS conducted in UKB data. The y axis shows a SNP's z statistic from applying MTAG to three GWAS of each trait conducted on equally sized subsamples of the baseline sample, in which every pair of samples had 50% overlap. **a**, Height. **b**, DEP. The figure illustrates near-perfect alignment. See the Supplementary Note for details and results from analogous analyses on additional phenotypes.

Estimation of Ω . We estimate $\hat{\Omega}$ by method of moments using the moment condition

$$E(\hat{\beta}_j \hat{\beta}_j' - \Omega - \Sigma_j) = 0$$

with $\hat{\Sigma}_j$ substituted in place of Σ_j . This is the step that relies on the assumption of homogeneous Ω : this assumption justifies using all SNPs when estimating $\hat{\Omega}$.

Summary. The MTAG results for SNP j are obtained in three steps: (i) estimate the variance–covariance matrix of the GWAS estimation error, $\hat{\Sigma}_j$, by using a sequence of LD score regressions, (ii) estimate the variance–covariance matrix of the SNP effects, $\hat{\Omega}$, using method of moments, and (iii) for each SNP, substitute these estimates into equation (1). We have made available for download a Python command line tool that runs our MTAG estimation procedure (see URLs). Because each of the above steps has a closed-form solution, genome-wide analyses using the MTAG software run quickly (Methods).

Theoretical analysis of MTAG's performance. This section briefly discusses three analytic formulas we have derived regarding the expected performance of MTAG for each trait: its MSE across SNPs, its statistical power to detect a true single-SNP association, and its FDR (Methods). All the formulas hold for an arbitrary number of traits. The Supplementary Note contains illustrative calculations.

The MSE formula is very general: it holds under any distribution of effect sizes, including distributions that violate the assumption of homogeneous Ω . The formula implies that, for each trait, the MTAG estimates always have a lower genome-wide MSE than corresponding GWAS estimates. This in turn suggests that polygenic predictors constructed from MTAG results are likely to outperform GWAS-based predictors very generally.

The power and FDR formulas (in contrast to the fully general MSE formula) assume that the true effect sizes, β_j , are drawn from some known mean-zero mixture of multivariate normal distributions. This class of distributions includes multivariate spike-and-slab distributions and other fat-tailed distributions that may be relevant in applications of MTAG.

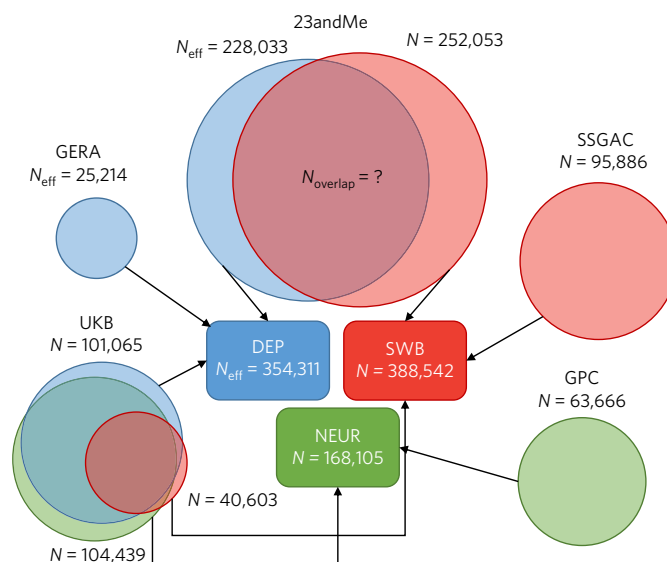


Fig. 3 | Cohorts included in GWAS meta-analyses for DEP, NEUR, and SWB. In UKB, the sample overlap in the summary statistics across the traits is known, whereas in 23andMe the sample overlap in the summary statistics is unknown. MTAG accounts for both sources of overlap. SSGAC results²⁰, GPC results¹⁹, GERA results¹⁸, and 23andMe results for DEP²¹ all come from previously published work. The data from 23andMe for SWB are newly analyzed data for this paper. Data from the UKB for all three traits have previously been published²⁰, although we reanalyzed them in this paper with slightly different protocols. N_{eff} is used instead of N when the cohort had case-control data (Supplementary Note). The sample size listed for each cohort corresponds to the maximum sample size across all SNPs available for that cohort. The total sample size for each trait corresponds to the maximum sample size among the SNPs available after applying MTAG filters. For details, see the Supplementary Note.

Potential biases in MTAG's test statistics. The derivation of MTAG relies on three important assumptions: (i) that Ω is homogeneous across SNPs, (ii) that sampling variation in $\hat{\Omega}$ and $\hat{\Sigma}_j$ can be ignored, and (iii) that the off-diagonal elements of $\hat{\Sigma}_j$ (estimated by bivariate LD score regression) accurately capture sample overlap. In light of each assumption, here we probe when and to what extent MTAG's test statistics for individual SNP associations may be biased.

Assumption of homogeneous Ω . If the assumption of homogeneous Ω is violated, then there are different types of SNPs with different Ω values. Because MTAG combines GWAS estimates using the genome-wide (i.e., across-SNP) variance–covariance matrix, in general MTAG estimates will be biased in finite samples. For the type of SNP that is null for one trait but non-null for other traits, the effect estimate on the first trait will be biased away from zero. For that reason, the FDR will be inflated.

Replication is the best way to assess the credibility of individual SNP associations. In addition, credibility can be probed using the FDR formula, computed under plausible assumptions about genetic architecture. In our application below, we calculate what we call 'maxFDR', which is an upper bound for the FDR under certain assumptions (Methods). In particular, we assume that the effect size distribution is a multivariate spike-and-slab distribution in which at least 10% of SNPs are non-null for each trait. Illustrative calculations indicate that a trait's maxFDR can be high when the GWAS for the trait is low powered while the GWAS for another trait is higher powered (Supplementary Note).

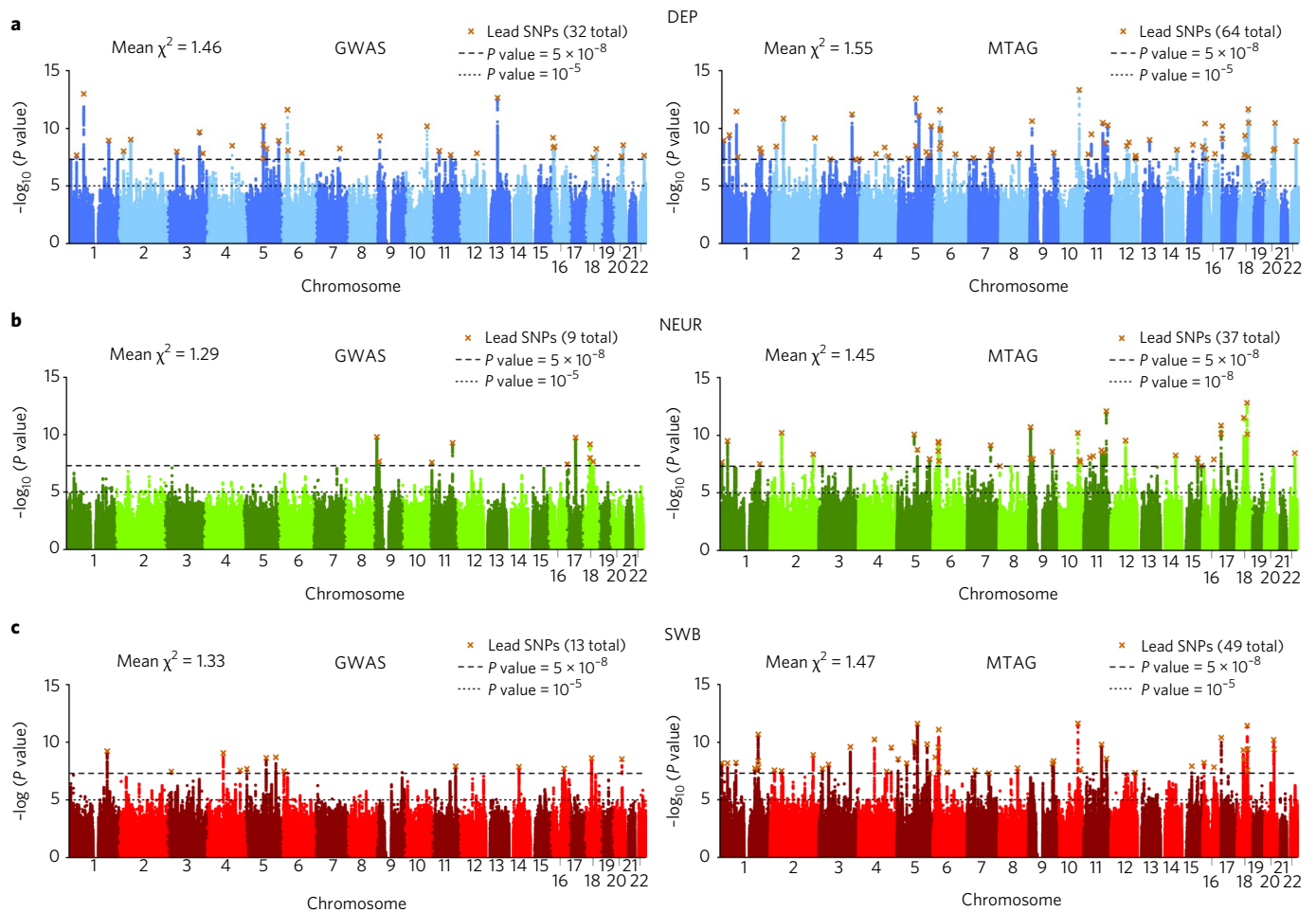


Fig. 4 | Manhattan plots of GWAS and MTAG results. a, DEP. b, NEUR. c, SWB. The left and right plots display the GWAS and MTAG results, respectively, for a fixed set of SNPs. The x axis shows chromosomal position, and the y axis shows significance on a $-\log_{10}$ scale. The upper dashed line marks the threshold for genome-wide significance ($P = 5 \times 10^{-8}$), and the lower line marks the threshold for suggestive significance ($P = 1 \times 10^{-5}$). Each approximately independent genome-wide significant association (lead SNP) is marked by a cross. The mean χ^2 statistic across all SNPs included in the analysis is displayed in the top left corner of each plot.

Ignored sampling variation in $\hat{\Omega}$ and $\hat{\Sigma}_j$. To assess the magnitude of the bias for finite samples in MTAG's standard errors from ignoring sampling variation in $\hat{\Omega}$ and $\hat{\Sigma}_j$, we simulated GWAS summary statistics for up to $T = 20$ traits and applied MTAG using $\hat{\Omega}$ and $\hat{\Sigma}_j$ (as in any real data application of MTAG). We then calculated the inflation of the mean χ^2 statistic, defined relative to what the mean χ^2 statistic would be if the true values Ω and Σ_j were used. The inflation is plotted as a function of T in Fig. 1a,b, where each GWAS has a mean χ^2 statistic of 1.1, 1.4, or 2.0. The effect size correlation for every pair of traits is $r_\beta = 0$ (Fig. 1a) or $r_\beta = 0.7$ (Fig. 1b); we set the correlation in estimation error for every pair of traits to $r_e = 0$ in these simulations. The figure shows that inflation increases roughly linearly with the number of traits. The bias is larger when the GWAS are lower powered and when r_β is smaller. Our application to DEP, NEUR, and SWB (discussed below) corresponds roughly to a mean χ^2 statistic of 1.4 with $T = 3$ in Fig. 1b. In that setting, inflation is negligible. Even when inflation is at its largest—for the low-powered GWAS with $T = 20$ in Fig. 1a—it is only 3%.

These simulations suggest that, in most realistic applications of MTAG, the bias from ignoring sampling variation in $\hat{\Omega}$ and $\hat{\Sigma}_j$ is negligibly small. A possible exception, not discussed so far, arises if MTAG is used for GWAS meta-analysis across a large number of cohorts (in which case T is large). MTAG may be valuable for

this purpose because (i) it accounts for sample overlap and cryptic relatedness across cohorts and (ii) different cohorts often have phenotypic data from different measures, which may be imperfectly genetically correlated and have different heritabilities. For such applications, to reduce bias in the MTAG standard errors, we recommend imposing reasonable parameter restrictions on the $\hat{\Omega}$ and $\hat{\Sigma}_j$ matrices (for example, assuming that within groups of cohorts that analyzed identical phenotype measures the heritability is equal and all pairwise genetic correlations are one).

$\hat{\Sigma}_j$ accurately captures sample overlap. MTAG relies on bivariate LD score regression (and, by extension, its assumptions) to estimate the correlation in GWAS estimation error due to sample overlap. To gauge MTAG's performance, we simulated an extreme case of sample overlap using real data from the UK Biobank (UKB). We ran three GWAS of height, each using two-thirds of the data, with 50% overlap between the samples for each pair of GWAS. Then, we ran MTAG on the three GWAS. A scatterplot of the resulting MTAG z statistics against the z statistics from a single GWAS run on the entire UKB sample is shown in Fig. 2a. The scatterplot from an analogous analysis of DEP in UKB is shown in Fig. 2b. The regression slope and coefficient of determination (R^2) are both essentially one for both phenotypes, indicating that MTAG generates the correct

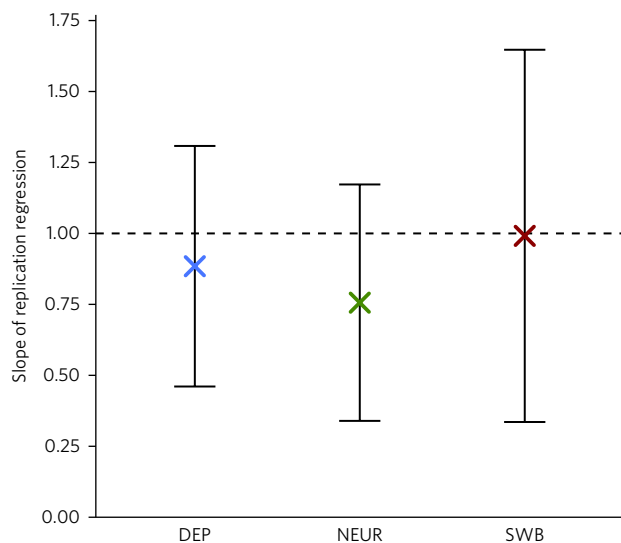


Fig. 5 | Regression-based test of the replicability of MTAG-identified loci.

For each trait and in each of two independent replication cohorts (HRS and Add Health; combined $N = 12,641$), we regressed the estimated effect sizes of the MTAG-identified loci on their winner's curse-adjusted MTAG effect sizes. The intercept is constrained to zero in these regressions. The plotted regression coefficients are the sample-size-weighted means across the replication cohorts, with 95% intervals. See the Supplementary Note for details and cohort-level results.

z statistics in these cases. The results were similar when we repeated this analysis using four other phenotypes (Methods).

GWAS summary statistics for depression, neuroticism, and subjective well-being. For our empirical application of MTAG, we built on a recent study by the Social Science Genetic Association Consortium (SSGAC) of three traits that have been found to be highly polygenic and strongly genetically related: DEP, NEUR, SWB. In these analyses, we combined data from the largest previously published studies^{7–9,11} with new genome-wide analyses from the genetic testing company 23andMe, Inc., and the first release of UKB data. As depicted in Fig. 3, there was substantial overlap between the estimation samples for the three traits (for additional details, see the Methods and Supplementary Note).

MTAG results. We applied MTAG to the summary statistics from the three single-trait analyses described above. To enable a fair comparison between the MTAG and GWAS results, we restricted all analyses to a common set of SNPs (see the Methods for details and recommended filters for MTAG).

Manhattan plots from the GWAS and MTAG analyses for each trait are shown side by side in Fig. 4. Approximately independent genome-wide significant SNPs, hereafter referred to as 'lead SNPs', were defined by clumping with an r^2 threshold of 0.1, where r^2 is the squared correlation between a pair of SNP genotypes (Methods). From GWAS to MTAG, the number of lead SNPs increased from 32 to 64 for DEP, from 9 to 37 for NEUR, and from 13 to 49 for SWB.

For the MTAG hits, we calculated the maxFDR assuming that at least 10% of SNPs were non-null for each trait (our estimates of the actual percentage that was not null were 59–65% across the three traits; Methods). The maxFDR was 0.0014 for DEP, 0.0080 for NEUR, and 0.0044 for SWB. This calculation suggests that the hits are unlikely to be an artifact of the assumption of homogeneous Ω .

For each trait, we assessed the gain in average power for MTAG relative to the GWAS results by the increase in the mean χ^2 statistic.

We used this increase to calculate how much larger the GWAS sample would have to be to attain an equivalent increase in the expected χ^2 statistic (Methods). We found that the MTAG analysis of DEP, NEUR, and SWB yielded gains equivalent to augmenting the original samples by 27%, 55%, and 55%, respectively. The resulting GWAS-equivalent sample sizes were thus 449,649 for DEP, 260,897 for NEUR, and 600,834 for SWB.

Replication of MTAG-identified loci. To test the lead SNPs for replication, we used the Health and Retirement Study (HRS) and the National Longitudinal Study of Adolescent to Adult Health (Add Health), which both contain high-quality measures of DEP, NEUR, and SWB. Because HRS was included in the SSGAC discovery sample for SWB, we reran the GWAS and MTAG analyses for SWB after omitting it. Although our replication samples were too small for well powered replication analyses of single-SNP associations, we were adequately powered to test the SNPs jointly. For the set of MTAG-identified lead SNPs for each trait, we regressed the effect sizes in HRS and in Add Health on the MTAG effect sizes, after correcting the MTAG effect size estimates for winner's curse (Supplementary Note). The regression slopes for the two replication cohorts were then meta-analyzed. If the SNP effect sizes taken all together replicate, then we expect a slope of one. The regression slopes were 0.88 (standard error (s.e.) = 0.22) for DEP, 0.76 (s.e. = 0.21) for NEUR, and 0.99 (s.e. = 0.33) for SWB (Fig. 5). In all cases, the slope was statistically significantly greater than zero (one-sided $P = 2.16 \times 10^{-5}$, 1.87×10^{-4} , and 1.52×10^{-3} , respectively) but not statistically distinguishable from one.

Polygenic prediction. We next compared the predictive power of polygenic scores constructed from GWAS versus MTAG association statistics. We again used the HRS and Add Health cohorts as our prediction samples (and obtained the SNP effect estimates for SWB from the analyses that omitted HRS from the discovery sample).

We measured the predictive power of each polygenic score by its incremental R^2 value, defined as the increase in R^2 as we moved from a regression of the trait only on a set of controls (year of birth, year of birth squared, sex, interactions of these variables, and ten principal components of the genetic data) to a regression that additionally included the polygenic score as an independent variable.

The results from our pooled analysis of Add Health and HRS are shown in Fig. 6 and Table 1. The GWAS-based polygenic scores had incremental R^2 values of 1.00% for DEP, 1.27% for NEUR, and 1.20% for SWB. The corresponding MTAG-based polygenic scores all had greater predictive power: 1.17% for DEP, 1.65% for NEUR, and 1.57% for SWB. The proportional improvement in incremental R^2 values was in the range of 17–30% for each trait, with 95% confidence intervals that did not overlap zero. The absolute levels of predictive power were clearly too small to be of clinical utility, but the improvements in R^2 values were close to those we would expect theoretically on the basis of the observed increases in mean χ^2 statistics (Methods). Polygenic scores based on trait-specific MTAG results had greater predictive power than scores based on MTAG results for the other traits (Fig. 6c,d), consistent with the theoretical result that MTAG results can be interpreted as trait-specific estimates.

Biological annotation. For a final comparison, we analyzed both the GWAS and MTAG results using the bioinformatics tool DEPICT¹⁵. We present the prioritized genes, enriched gene sets, and enriched tissues identified by DEPICT at the standard FDR threshold of 5%.

The results are summarized in Table 1. In the GWAS-based analysis, very little enrichment was apparent. For DEP, three genes were identified, but no gene sets and only ten tissues. For NEUR and SWB, no genes, gene sets, or tissues were identified. In contrast, the MTAG-based analysis was more informative. The strongest results

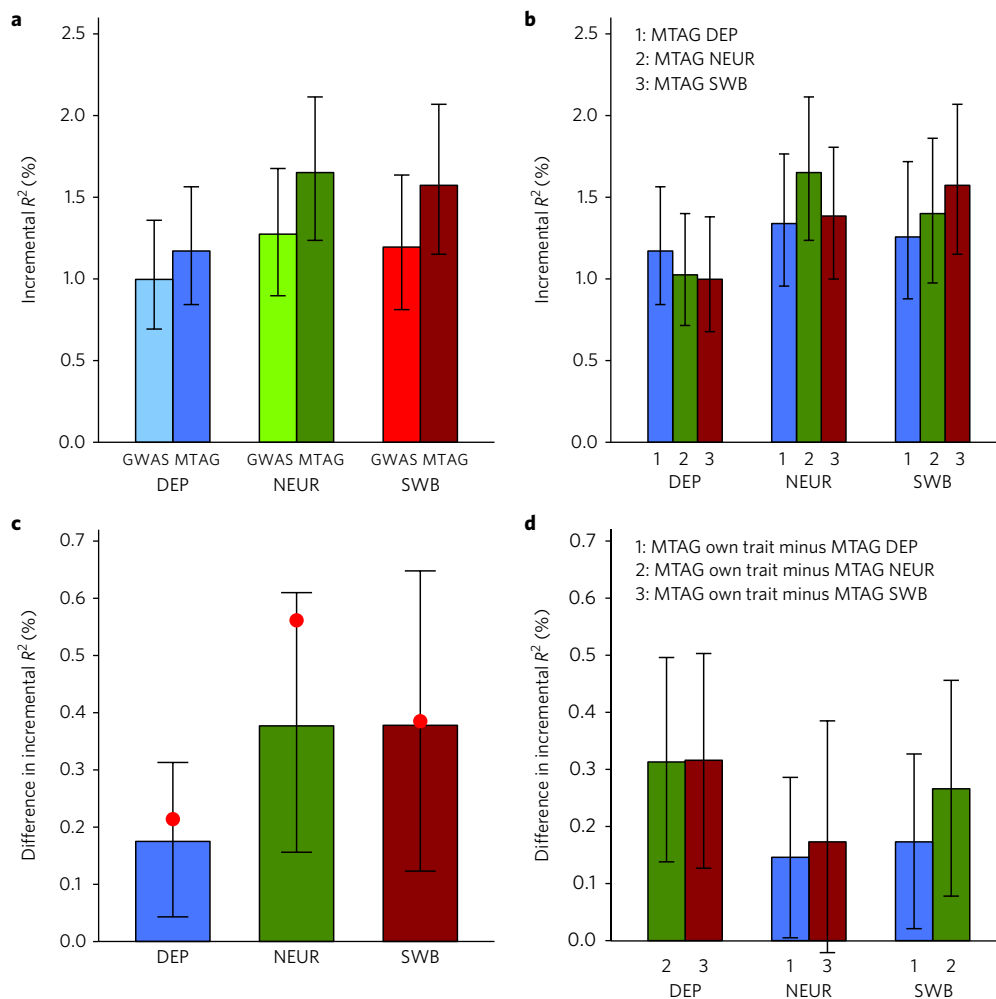


Fig. 6 | Predictive power of GWAS- and MTAG-based polygenic scores. Incremental R^2 is the increase in R^2 from a linear regression of the trait on the polygenic score and covariates, relative to a linear regression of the trait on only covariates. The plotted incremental R^2 (and differences in incremental R^2) are the sample-size-weighted means across the replication cohorts (HRS and Add Health; combined $N=12,641$), with 95% confidence intervals. See the Supplementary Note for details and cohort-level results. **a**, Incremental R^2 of MTAG-based and GWAS-based polygenic scores. **b**, Incremental R^2 of polygenic scores constructed from the MTAG results for the predicted trait (own trait score) or MTAG results for each of the other traits (other trait score). The x axis shows the trait being predicted, and bar color indicates which trait's polygenic score was used. **c**, Difference in incremental R^2 between the GWAS- and MTAG-based polygenic scores. Red dots indicate the theoretically predicted gains in prediction accuracy (Methods). **d**, Difference in incremental R^2 between own trait scores and the mean of the incremental R^2 from the other trait scores.

Table 1 | Summary of comparative analyses of GWAS and MTAG results

	DEP		NEUR		SWB	
	GWAS	MTAG	GWAS	MTAG	GWAS	MTAG
SNP-based comparisons						
Lead SNPs ($P < 5 \times 10^{-8}$)	32	64	9	37	13	49
Mean χ^2	1.43	1.55	1.29	1.45	1.30	1.47
N_{eff}	354,861	449,649	168,105	260,897	388,538	600,834
Polygenic score incremental R^2 (%)	1.00	1.17	1.27	1.65	1.20	1.57
Biological annotation (DEPICT FDR < 0.05)						
No. prioritized genes	3	72	0	51	0	0
No. gene sets	0	347	0	1	0	7
No. tissues and cell types	10	22	0	21	0	12

were again for DEP, now with 72 genes, 347 gene sets, and 22 tissues. For NEUR, there were 51 genes, 1 gene set, and 21 tissues, and for SWB there were zero genes, 7 gene sets, and 12 tissues.

For brevity, we discuss the specific results only for DEP; the results for NEUR and SWB were similar but more limited. For the tissues tested by DEPICT, Fig. 7a plots the P values based on both

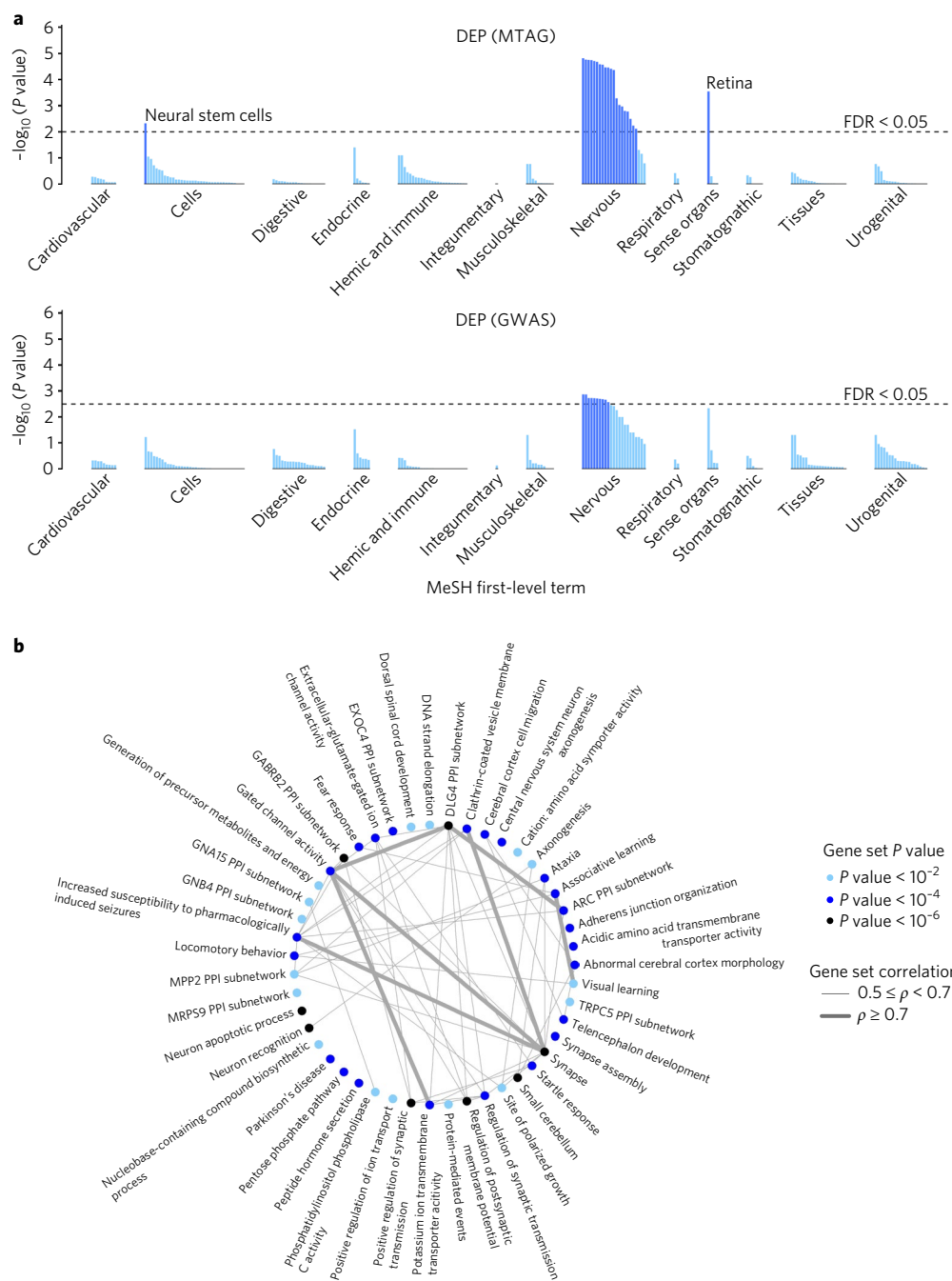


Fig. 7 | Biological annotation for DEP using the bioinformatics tool DEPICT. **a**, Results of the tissue enrichment analysis based on the GWAS and MTAG results. The x axis lists the tissues tested for enrichment, grouped by location of the tissue. The y axis shows statistical significance on a $-\log_{10}$ scale. The horizontal dashed line corresponds to an FDR of 0.05, which was the threshold used to identify prioritized tissues. **b**, Gene set clusters as defined by the Affinity Propagation algorithm²³ over the gene sets from the MTAG results. The algorithm names clusters after an exemplary member of the gene set. The color of each point signifies the P value of the most significant gene set in the cluster. The thickness of the lines between gene set clusters corresponds to the correlation between the named gene sets for each pair of clusters.

the GWAS and MTAG results. As expected, nearly all of the enrichment of signal was found in the nervous system. To facilitate interpretation of the enriched gene sets, we used a standard procedure¹⁶ to group the 347 gene sets into ‘clusters’ defined by degree of gene overlap. Many of the 46 resulting clusters, shown in Fig. 7b, implicate communication between neurons (‘synapse’, ‘synapse assembly’, ‘regulation of synaptic transmission’, ‘regulation of postsynaptic membrane potential’). This evidence is consistent with that from the DEPICT-prioritized genes, many of which encode proteins that

are involved in synaptic communication. For example, *PCLO*, *BSN*, *SNAP25*, and *CACNA1E* all encode important parts of the machinery that releases neurotransmitter from the signaling neuron¹⁷.

The results include some intriguing findings. For example, while hypotheses regarding major depression and related traits have tended to focus on monoamine neurotransmitters, our results as a whole point much more strongly to glutamatergic neurotransmission. Moreover, the particular glutamate receptor genes prioritized by DEPICT (*GRIK3*, *GRM1*, *GRM5*, and *GRM8*)

suggest the importance of processes involving communication between neurons on an intermediate time scale^{18,19}, such as learning and memory. Such processes are also implicated by many of the enriched gene sets, which relate to altered reactions to stress and novelty in mice (for example, 'decreased exploration in a new environment', 'increased anxiety-related response', 'behavioral fear response').

Comparison to other multi-trait methods. We compared MTAG to three multi-trait methods that can be applied to an arbitrary number of GWAS summary statistics with unknown overlap between them^{12,13} (Supplementary Note). Unlike MTAG, these methods do not provide trait-specific SNP effect estimates but instead test whether the SNP is associated with none of the traits. We generated a (conservative) MTAG-based test of the same null hypothesis by using the minimum of the trait-specific MTAG *P* values, Bonferroni adjusted for the number of traits. In two-trait simulations, we found that MTAG had greater power when the correlation in true effect sizes or GWAS estimation error was nonzero, especially when the GWAS for the traits were higher powered. In real data applications to (i) DEP, NEUR, and SWB and (ii) six anthropometric traits, MTAG identified more loci. We tested the anthropometric trait-associated loci in GIANT Consortium results and found that the loci identified by MTAG and missed by the other methods replicated at a higher rate than the loci identified by one of the other methods and missed by MTAG.

Discussion

We have introduced MTAG, a method for conducting meta-analysis of GWAS summary statistics for different traits that is robust to sample overlap. Both our theoretical and empirical results confirm that MTAG can increase the statistical power to identify trait-specific genetic associations. In our empirical application to DEP, NEUR, and SWB, we found that, relative to the separate GWAS for the traits, MTAG led to substantial improvements in the number of loci identified, the predictive power of polygenic scores, and the informativeness of a bioinformatics analysis. Table 1 summarizes the gains from MTAG across these analyses.

Because summary statistics from large-scale GWAS are accessible for an ever-increasing number of traits and tools are now available for using summary statistics to easily identify clusters of genetically correlated traits²⁰, there will be many sets of traits to which MTAG could be applied. Which potential applications will be most fruitful? Our theoretical results indicate that, relative to single-trait GWAS, MTAG will improve polygenic prediction quite generally. For identifying individual associated loci, MTAG will yield the greatest gains in statistical power and little inflation of the FDR for traits with high genetic correlation. We caution, however, that the FDR can become substantial if MTAG is applied to a large number of low-powered GWAS or to GWAS that differ a great deal in power—conditions that did not apply to our empirical application here. In all applications of MTAG, we recommend conducting FDR calculations and, of course, conducting replication analyses if possible.

Methods

Methods, including statements of data availability and any associated accession codes and references, are available at <https://doi.org/10.1038/s41588-017-0009-4>.

Received: 20 March 2017; Accepted: 6 November 2017;
Published online: 01 January 2018

References

- Galesloot, T. E., van Steen, K., Kiemeny, L. A., Jans, L. L. & Vermeulen, S. H. A comparison of multivariate genome-wide association methods. *PLoS One* **9**, e95923 (2014).
- Porter, H. F. & O'Reilly, P. F. Multivariate simulation framework reveals performance of multi-trait GWAS methods. *Sci. Rep.* **7**, 38837 (2017).
- Maier, R. et al. Joint analysis of psychiatric disorders increases accuracy of risk prediction for schizophrenia, bipolar disorder, and major depressive disorder. *Am. J. Hum. Genet.* **96**, 283–294 (2015).
- Hu, Y. et al. Joint modeling of genetically correlated diseases and functional annotations increases accuracy of polygenic risk prediction. *PLoS Genet.* **13**, e1006836 (2017).
- Baselmans, B.M.L. et al. Multivariate genome-wide and integrated transcriptome and epigenome-wide analyses of the well-being spectrum. Preprint at *bioRxiv* <https://doi.org/10.1101/115915> (2017).
- Bulik-Sullivan, B. et al. An atlas of genetic correlations across human diseases and traits. *Nat. Genet.* **47**, 1236–1241 (2015).
- Hyde, C. L. et al. Identification of 15 genetic loci associated with risk of major depression in individuals of European descent. *Nat. Genet.* **48**, 1031–1036 (2016).
- Ripke, S. et al. A mega-analysis of genome-wide association studies for major depressive disorder. *Mol. Psychiatry* **18**, 497–511 (2013).
- de Moor, M. H. M. et al. Meta-analysis of genome-wide association studies for neuroticism, and the polygenic association with major depressive disorder. *JAMA Psychiatry* **72**, 642–650 (2015).
- Smith, D. J. et al. Genome-wide analysis of over 106 000 individuals identifies 9 neuroticism-associated loci. *Mol. Psychiatry* **21**, 749–757 (2016).
- Okbay, A. et al. Genetic variants associated with subjective well-being, depressive symptoms, and neuroticism identified through genome-wide analyses. *Nat. Genet.* **48**, 624–633 (2016).
- Bolormaa, S. et al. A multi-trait, meta-analysis for detecting pleiotropic polymorphisms for stature, fatness and reproduction in beef cattle. *PLoS Genet.* **10**, e1004198 (2014).
- Zhu, X. et al. Meta-analysis of correlated traits via summary statistics from GWASs with an application in hypertension. *Am. J. Hum. Genet.* **96**, 21–36 (2015).
- Bulik-Sullivan, B. K. et al. LD Score regression distinguishes confounding from polygenicity in genome-wide association studies. *Nat. Genet.* **47**, 291–295 (2015).
- Pers, T. H. et al. Biological interpretation of genome-wide association studies using predicted gene functions. *Nat. Commun.* **6**, 5890 (2015).
- Frey, B. J. & Dueck, D. Clustering by passing messages between data points. *Science* **315**, 972–976 (2007).
- Südhof, T. C. The presynaptic active zone. *Neuron* **75**, 11–25 (2012).
- Pin, J.-P. & Bettler, B. Organization and functions of mGlu and GABA_B receptor complexes. *Nature* **540**, 60–68 (2016).
- Traynelis, S. F. et al. Glutamate receptor ion channels: structure, regulation, and function. *Pharmacol. Rev.* **62**, 405–496 (2010).
- Zheng, J. et al. LD Hub: a centralized database and web interface to perform LD score regression that maximizes the potential of summary level GWAS data for SNP heritability and genetic correlation analysis. *Bioinformatics* **33**, 272–279 (2017).
- Yang, J., Lee, S. H., Goddard, M. E. & Visscher, P. M. GCTA: a tool for genome-wide complex trait analysis. *Am. J. Hum. Genet.* **88**, 76–82 (2011).

Acknowledgements

We thank J. Beauchamp, P. Koellinger, Ö. Sandewall, C. Shulman, and R. de Vlaming for helpful comments and P. Bowers, E. Kong, T. Kundu, S. Lee, H. Li, R. Li, and R. Royer for research assistance. This research was carried out under the auspices of the Social Science Genetic Association Consortium (SSGAC). The study was supported by the Ragnar Söderberg Foundation (E9/11, M.J.; E42/15, D.C.), the Swedish Research Council (421-2013-1061, M.J.), the Jan Wallander and Tom Hedelius Foundation (M.J.), an ERC Consolidator Grant (647648 EdGe, P. Koellinger), the Pershing Square Fund of the Foundations of Human Behavior (D.L.), the National Science Foundation's Graduate Research Fellowship Program (DGE 1144083, R.W.), and the NIA/NIH through grants P01-AG005842, P01-AG005842-20S2, and T32-AG000186-23 to D. Wise at NBER; P30-AG012810 (D.L.) to NBER; R01-AG042568-02 (D.J.B.) to the University of Southern California; and 1R01-MH107649-03 (B.M.N.), 1R01-MH101244-02 (B.M.N.), and 5U01-MH109539-02 (B.M.N.) to the Broad Institute at Harvard and MIT. This research has also been conducted using the UK Biobank Resource under application number 11425. We thank the research participants and employees of 23andMe for making this work possible. We also thank K. Mullan Harris and Add Health for early access to the data used in our replication and prediction analyses. A full list of acknowledgements is provided in the Supplementary Note.

Author Contributions

B.M.N., D.J.B., D.C., and P.T. oversaw the study. The theory underlying MTAG was conceived of and developed by P.T., with contributions from B.M.N., D.J.B., D.C., D.L., O.M., P.M.V., and R.K.W. O.M., P.T., and R.K.W. performed the simulations and

developed the MTAG software. P.T. and P.M.V. designed the analyses comparing the observed MTAG gains to theoretical expectations. A.O., M.Z., R.W., M.A.F., O.M., and T.A.N.-V. had major roles in data analyses. J.J.L. designed and executed the bioinformatics analyses. N.A.F. conducted the analysis of the data from 23andMe. D.J.B., D.C., and P.T. coordinated the writing of the manuscript. P.M., S.O., and M.J. also contributed to the writing. All authors provided input and revisions for the final manuscript.

Competing interests

The authors declare no competing financial interests.

Additional information

Supplementary information is available for this paper at <https://doi.org/10.1038/s41588-017-0009-4>.

Reprints and permissions information is available at www.nature.com/reprints.

Correspondence and requests for materials should be addressed to P.T. or D.C. or B.M.N. or D.J.B.

Publisher's note: Springer Nature remains neutral with regard to jurisdictional claims in published maps and institutional affiliations.

23andMe Research Team:

Michelle Agee¹², Babak Alipanahi¹², Adam Auton¹², Robert K. Bell¹², Katarzyna Bryc¹², Sarah L. Elson¹², Pierre Fontanillas¹², Nicholas A. Furlotte¹², David A. Hinds¹², Bethann S. Hromatka¹², Karen E. Huber¹², Aaron Kleinman¹², Nadia K. Litterman¹², Matthew H. McIntyre¹², Joanna L. Mountain¹², Carrie A. M. Northover¹², J. Fah Sathirapongsasuti¹², Olga V. Sazonova¹², Janie F. Shelton¹², Suyash Shringarpure¹², Chao Tian¹², Joyce Y. Tung¹², Vladimir Vacic¹², Catherine H. Wilson¹² and Steven J. Pitts¹²

Methods

This article is accompanied by a Supplementary Note with further details.

Theory. There are T traits, which may be binary or quantitative. We standardize each trait and the genotype for each SNP j so that they all have mean zero and variance one. The length- T vector of marginal (i.e., not controlling for other SNPs) true effects of SNP j in each of the traits is denoted as β_j . We assume that these are random effects with mean zero and variance-covariance matrix Ω that is the same across j . The mean is zero because we treat the choice of reference allele as arbitrary. We make the common assumption^{14,21,22} that the β_j values are identically distributed across j . The assumption implies that the expected amount of phenotypic variance explained is equal for each SNP, regardless of SNP characteristics such as allele frequency.

The length- T vector of GWAS estimates is denoted $\hat{\beta}_j$, which is equal to the true effect vector plus estimation error, $\beta_j + \epsilon_j$. The estimation error is the sum of sampling variation and biases (such as population stratification or technical artifacts). With any standard GWAS estimator (such as OLS or logistic regression), sampling variation is uncorrelated with β_j . We assume that the biases are also uncorrelated with β_j . The variance-covariance matrix of ϵ_j , denoted Σ_j , may differ across SNPs j owing to differences in the SNPs' sample sizes per trait and the SNPs' sample overlap between traits, although we only account for the former in our estimation of Σ_j . MTAG is a generalized method of moments (GMM) estimator. To obtain the key moment conditions we will use, we consider the best linear prediction of the GWAS estimate for trait s , $\hat{\beta}_{j,s}$, from the SNP's true effect on trait t , $\beta_{j,t}$. We use a first-order condition of this best linear prediction as the moment condition for trait s

$$E\left(\hat{\beta}_{j,s} - \frac{\omega_{st}}{\omega_{tt}}\beta_{j,t}\right) = 0$$

where ω_{st} is the (s,t) th element of Ω . There are T such moment conditions for $s=1, 2, \dots, T$, giving us the vector of moment conditions

$$E\left(\hat{\beta}_j - \frac{\omega_t}{\omega_{tt}}\beta_{j,t}\right) = 0 \quad (2)$$

where ω_t is a vector equal to the t th column of Ω . Although $\beta_{j,t}$ is a random effect, we aim to estimate its (unknown) realized value. The efficient GMM estimator for $\beta_{j,t}$ based on the vector of moment conditions in equation (1) solves

$$\hat{\beta}_{\text{MTAG},j,t} = \arg \min_{\beta_{j,t}} \left(\hat{\beta}_j - \frac{\omega_t}{\omega_{tt}}\beta_{j,t} \right)' W_Q \left(\hat{\beta}_j - \frac{\omega_t}{\omega_{tt}}\beta_{j,t} \right) \quad (3)$$

where $W_Q = \left[\text{var}\left(\hat{\beta}_j - \frac{\omega_t}{\omega_{tt}}\beta_{j,t}\right) \right]^{-1} = \left(\Omega - \frac{\omega_t\omega_t'}{\omega_{tt}} + \Sigma_j \right)^{-1}$ is the efficient weight matrix.

Intuitively, the GMM estimator chooses the value of $\beta_{j,t}$ that minimizes a weighted sum of the squared deviations from the moment conditions, with deviations weighted more heavily if they are estimated more precisely. In the Supplementary Note, we show that the solution to the minimization problem in equation (3) is

$$\hat{\beta}_{\text{MTAG},j,t} = \frac{\frac{\omega_t'}{\omega_{tt}} \left(\Omega - \frac{\omega_t\omega_t'}{\omega_{tt}} + \Sigma_j \right)^{-1} \hat{\beta}_j}{\frac{\omega_t'}{\omega_{tt}} \left(\Omega - \frac{\omega_t\omega_t'}{\omega_{tt}} + \Sigma_j \right)^{-1} \frac{\omega_t}{\omega_{tt}}}$$

Standard asymptotic properties of GMM relate to $T \rightarrow \infty$. In the Supplementary Note, we show that for a fixed number of traits T , as the sample size for the GWAS of any trait t becomes large, the MTAG estimator $\hat{\beta}_{\text{MTAG},j,t}$ is consistent and asymptotically normal.

The sampling variance of the estimator is

$$\text{var}\left(\hat{\beta}_{\text{MTAG},j,t} - \beta_{j,t}\right) = \frac{1}{\frac{\omega_t'}{\omega_{tt}} \left(\Omega - \frac{\omega_t\omega_t'}{\omega_{tt}} + \Sigma_j \right)^{-1} \frac{\omega_t}{\omega_{tt}}}$$

For each trait t , the standard error of the estimate is the square root of this quantity. As is standard, we obtain a P value using the fact that, in large samples, $\hat{\beta}_{\text{MTAG},j,t}$ divided by its standard error follows a standard normal distribution under the null hypothesis.

Because of the homogeneous Ω assumption, the above formulas for the MTAG estimator and its standard error effectively use the variance-covariance matrix of true SNP effects across all SNPs, Ω , to calculate the MTAG estimate for each SNP. In fact there are different types of SNPs characterized by different variance-covariance matrices, then the MTAG estimator remains consistent but could be made more efficient if it took into account the different types of SNPs. In addition,

the standard error formula is conservative on average across SNPs, which reduces MTAG's statistical power to identify truly associated SNPs. Most importantly, the MTAG estimator is in general biased in finite samples, and it is biased away from zero for SNPs that are truly null, which causes the false positive rate to be inflated.

For each SNP j , treating Σ_j as known, the matrix Ω is estimated using the method of moments (see the Supplementary Note for discussion of the relationship to GMM). For each (t,s) th entry of Ω , ω_{ts} , we use the moment condition $E\left(\hat{\beta}_{j,t}\hat{\beta}_{j,s} - \omega_{ts} - \Sigma_{j,ts}\right) = 0$. This moment condition is derived from observing that $E\left(\hat{\beta}_{j,t}\hat{\beta}_{j,s}\right) = E\left[\left(\beta_{j,t} + \epsilon_{j,t}\right)\left(\beta_{j,s} + \epsilon_{j,s}\right)\right] = E\left[\beta_{j,t}\beta_{j,s}\right] + E\left[\epsilon_{j,t}\epsilon_{j,s}\right] = \omega_{ts} + \Sigma_{j,ts}$. The estimator simply replaces the population expectation with the sample mean

$$\hat{\omega}_{ts} = \frac{1}{M} \sum_{m=1}^M \hat{\beta}_{j,t} \hat{\beta}_{j,s} - \Sigma_{j,ts}$$

where M is the number of SNPs in the analysis. Intuitively, the estimated covariance in true genetic effects between trait t and trait s is equal to the covariance in their observed GWAS coefficients minus the covariance in GWAS coefficients that is due to correlated estimation error.

For expositional simplicity, our derivations above and in the Supplementary Note are parameterized in terms of the parameter vector $\hat{\beta}_j$. We note, however, that the input to the MTAG software is the standard output from meta-analysis software: z statistics and sample sizes. Because MTAG is applied to z statistics, the GWAS summary statistics do not need to have been estimated using traits and genotypes that were standardized.

Special cases. There are three special cases of MTAG that may often be relevant in practice and for which the estimation procedure is made faster and more efficient. The MTAG software offers the option to specialize the analysis for these cases.

No sample overlap across traits. In this case, the off-diagonal elements of Σ_j can be set equal to zero, so LD score regression needs to be run only T rather than $T(T+1)/2$ times. Note that this version of MTAG does not take into account correlation in estimation error across traits that is due to bias. For this reason, LD score regression should be run on the MTAG results, and the resulting MTAG standard errors should be inflated by the square root of the estimated intercept.

Perfect genetic correlation but different heritabilities. This case arises when the 'traits' are different measures of the same trait, some with more measurement error than others, or when the variance in the trait due to non-genetic factors differs. Here the Ω matrix has only T rather than $T(T+1)/2$ unique parameters to be estimated.

Perfect genetic correlation and equal heritabilities. This special case corresponds to the 'traits' being (the same measure of) a single trait; in other words, applying MTAG instead of inverse-variance-weighted meta-analysis to T GWAS results. Doing so can be useful if there is sample overlap in the GWAS results. In this case, as noted in the main text, MTAG specializes to $\hat{\beta}_{\text{MTAG},j,t} = \frac{1}{1 + \Sigma_j^{-1}} \hat{\beta}_j$ for all t and it is no longer necessary to estimate Ω .

MTAG's genome-wide mean squared error. The genome-wide mean squared error (MSE) of the MTAG estimates is simply equal to their sampling variance (given above)

$$\begin{aligned} \text{MSE}\left(\hat{\beta}_{\text{MTAG},j,t}\right) &\equiv E\left[\left(\hat{\beta}_{\text{MTAG},j,t} - \beta_{j,t}\right)^2\right] \\ &= \text{var}\left(\hat{\beta}_{\text{MTAG},j,t} - \beta_{j,t}\right) = \frac{1}{\frac{\omega_t'}{\omega_{tt}} \left(\Omega - \frac{\omega_t\omega_t'}{\omega_{tt}} + \Sigma_j \right)^{-1} \frac{\omega_t}{\omega_{tt}}} \end{aligned}$$

where the first equality follows because both the true effects $\beta_{j,t}$ and the MTAG estimates $\hat{\beta}_{\text{MTAG},j,t}$ are mean zero. Illustrative calculations of this formula in a two-trait setting are shown in Supplementary Fig. 1. This formula for the MSE holds very generally; in particular, it does not require assuming that Ω is homogeneous across SNPs (because the genome-wide MSE is a property regarding the mean across all the SNPs included in the analysis). In the formula, Ω is (re)defined as the genome-wide (i.e., across-SNP) variance-covariance matrix of the SNPs' true effects on the traits. By simulation, we verify that the MSE formula is a good approximation when using estimates of Ω and Σ_j (Supplementary Table 1).

In the Supplementary Note, we show that the MSE values of the MTAG estimates are always smaller than the MSE of the corresponding single-trait GWAS estimates, which equals $\text{MSE}\left(\hat{\beta}_{j,t}\right) \equiv E\left[\left(\hat{\beta}_{j,t} - \beta_{j,t}\right)^2\right] = E\left(\epsilon_{j,t}^2\right)$. Intuitively, this result holds because the MTAG estimates have smaller variance than the GWAS estimates and both are unbiased on average across all SNPs; the MTAG estimates are unbiased on average (despite being biased for particular SNPs when the homogeneous Ω assumption is violated) because both the true effects $\beta_{j,t}$ and the MTAG estimates $\hat{\beta}_{\text{MTAG},j,t}$ are mean zero across SNPs.

MTAG's power and false discovery rate when effect sizes are mixture-normal distributed. Suppose that the vector of SNP j 's effects on the traits β_j is drawn from a mixture of mean-zero multivariate normal distributions. The distribution of component $c = 1, 2, \dots, C$ is $\beta_j | c \sim N(\mathbf{0}, \Omega_c)$ and its mixture weight is denoted p_c , where $\sum_{c=1}^C p_c = 1$. In this case, the z statistic associated with the MTAG estimate $\hat{\beta}_{\text{MTAG},j,t}$ is a mixture distribution with component distributions

$$Z_{j,t}|c \sim N\left(\mathbf{0}, \frac{\frac{\omega'_t}{\omega_{tt}}\left(\Omega - \frac{\omega\omega'_t}{\omega_{tt}} + \Sigma_j\right)^{-1}\left(\Omega_c + \Sigma_j\right)\left(\Omega - \frac{\omega\omega'_t}{\omega_{tt}} + \Sigma_j\right)^{-1}\frac{\omega_t}{\omega_{tt}}}{\frac{\omega'_t}{\omega_{tt}}\left(\Omega - \frac{\omega\omega'_t}{\omega_{tt}} + \Sigma_j\right)^{-1}\frac{\omega_t}{\omega_{tt}}}\right)$$

To define power and FDR, let D denote the set of components such that a SNP is null for trait t , i.e., the t th element of β_j is drawn from a degenerate distribution with all mass on zero. Power for trait t can be calculated as

$$\text{Power} \equiv \Pr\left(\left|Z_{j,t}\right| > z_0 \mid c \notin D\right) = \frac{\sum_{c \notin D} \Pr\left(\left|Z_{j,t}\right| > z_0 \mid c\right) p_c}{\sum_{c \notin D} p_c}$$

where z_0 is the z statistic associated with genome-wide significance. The FDR for trait t can be calculated as

$$\begin{aligned} \text{FDR} &\equiv \Pr\left(\text{null} \mid \left|Z_{j,t}\right| > z_0\right) \\ &= \frac{\Pr\left(\left|Z_{j,t}\right| > z_0 \mid \text{null}\right) \Pr(\text{null})}{\Pr\left(\left|Z_{j,t}\right| > z_0\right)} \\ &= \frac{\sum_{c \in D} \Pr\left(\left|Z_{j,t}\right| > z_0 \mid c\right) p_c}{\sum_{c=1}^C \Pr\left(\left|Z_{j,t}\right| > z_0 \mid c\right) p_c} \end{aligned}$$

As with the MSE formula, we verify in simulations that these formulas are good approximations when using estimates of Ω and Σ_j (Supplementary Table 1).

Maximum FDR when effect sizes are multivariate spike-and-slab distributed. Starting with the mixture-normal setup in the derivation of power and the FDR, we assume that there are $C = 2^T$ components, corresponding to all possible combinations of the SNP being null for some subset of traits and non-null for the others. Let $\tilde{\Omega}$ denote the variance-covariance matrix of true effect sizes for the component in which the SNP is non-null for all the traits. We assume that the variance-covariance matrix of true effect sizes for any component c , denoted Ω_c , is equal to $\tilde{\Omega}$ but with the rows and columns zeroed out that correspond to null traits in component c . Given our estimate of $\tilde{\Omega}$, for any vector of mixing weights $\mathbf{p} = (p_1, p_2, \dots, p_C)$, to construct an estimate of $\tilde{\Omega}$, we set the (t,s) th entry of $\tilde{\Omega}(\mathbf{p})$ equal to $\tilde{\omega}_{ts}(\mathbf{p}) = \frac{\omega_{ts}}{\sum_{c \in E_{t,s}} p_c}$ where $E_{t,s}$ is the set of components in which the SNP is non-null for both traits t and s . We call the mixing weights \mathbf{p} 'feasible' if the resulting matrix $\tilde{\Omega}(\mathbf{p})$ is positive semidefinite. We maximize the FDR (given by the formula above) over all feasible mixing weights \mathbf{p} . Given that the FDR may not be a unimodal function of \mathbf{p} , we maximize using a grid search. Because \mathbf{p} has 2^T elements, it may be computationally infeasible to perform a fine grid search when T is larger than three or four. Illustrative calculations of maxFDR in a two-trait setting are shown in Supplementary Fig. 2.

Evaluation of MTAG's robustness to sample overlap. Using the same procedure described in the main text (and in further detail in the Supplementary Note), we also tested the robustness of MTAG to sample overlap using four other traits available in the UKB: body mass index, educational attainment, neuroticism, and subjective well-being. The results are qualitatively the same as those based on height (Supplementary Fig. 3).

Simulations. To speed computations, instead of simulating individual-level data and then estimating effect sizes, we directly generated effect size estimates by adding multivariate normally distributed noise to the simulated effect sizes. The variance of the noise for each trait was determined by the assumed GWAS expected χ^2 statistics, and the covariance of the noise between the traits was determined by the assumed GWAS expected χ^2 statistics and correlation of GWAS estimation error across traits.

In our simulations, we cannot estimate Σ_j using LD score regressions because we directly simulate effect sizes rather than data. Nonetheless, we would like to use a matrix for $\tilde{\Sigma}_j$ that contains the same amount of sampling variance that would have been present if we had simulated data and then run LD score regressions. To accomplish this, in each replication, we directly generated $\tilde{\Sigma}_j$

by adding noise to the true value of Σ_j . The variance of the noise was calibrated against the LD score regression intercept standard errors for the GWAS results of DEP, NEUR, and SWB that we estimated in our empirical application but scaled to be larger or smaller when the simulated GWAS had more power (Supplementary Note).

GWAS meta-analyses of DEP, NEUR, and SWB. Details on the cohorts, phenotype measures, genotyping, quality control filters, and association models are provided in the Supplementary Note and Supplementary Tables 2–5. As shown in Fig. 3, there is substantial overlap in samples across the three GWAS meta-analyses.

All analyses were based on autosomal SNPs from cohorts with genotypes imputed against the 1000 Genomes reference panel. The input files in each meta-analysis were subjected to a uniform set of quality control and diagnostic procedures. These are described in the previous SSGAC study¹¹ and the Supplementary Note.

As expected under polygenicity²³, we observed inflation of the median test statistic in each GWAS ($\lambda_{\text{GC,DEP}} = 1.36$, $\lambda_{\text{GC,NEUR}} = 1.24$, $\lambda_{\text{GC,SWB}} = 1.28$; Supplementary Fig. 4 and Supplementary Table 6). The intercept estimates from LD score regression were all below 1.02, however, suggesting that nearly all of the observed inflation is due to polygenic signal¹⁴ (Supplementary Fig. 5). When we report GWAS results, as in the SSGAC study¹¹, we account for the potential bias due to this small amount of stratification by inflating the standard errors of our GWAS estimates by the square root of the LD score regression intercept.

Manhattan plots from each of the GWAS meta-analyses are shown in Supplementary Fig. 6. Our NEUR meta-analysis was based on the same cohort-level data as the SSGAC study¹¹ and unsurprisingly yielded substantively identical results: ten lead SNPs. Consistent with what studies have reported for other complex traits, the larger discovery samples for DEP and SWB relative to the SSGAC study increased the number of lead SNPs: from 2 to 32 for DEP ($N_{\text{eff}} = 149,707$ to 354,862) and from 3 to 13 for SWB ($N = 298,420$ to 388,538). Applying bivariate LD score regression⁶ to the GWAS results, we estimated the genetic correlations to be 0.72 (s.e. = 0.026) between DEP and NEUR, -0.67 (s.e. = 0.027) between NEUR and SWB, and -0.69 (s.e. = 0.024) between DEP and SWB (Supplementary Table 7). The intercepts from each of these regressions are found in Supplementary Table 8. Lead SNPs with a P value less than 1×10^{-5} from the GWAS for each trait are listed in Supplementary Table 9.

Clumping algorithm. We applied the same clumping algorithm to the GWAS and MTAG results to identify each set of lead SNPs. Our clumping algorithm is the same as in the previous SSGAC study¹¹. First, the SNP with the smallest P value was identified in the meta-analysis results. This SNP was designated the index SNP of clump 1. Second, we identified all SNPs on the same chromosome whose LD with the index SNP exceeded $r^2 = 0.1$ and assigned them to clump 1. To generate the second clump, we removed the SNPs in clump 1 and then iterated the process to identify further index SNPs and their corresponding clumps until no SNPs remained.

MTAG SNP filters. Because the derivation of MTAG relies on some assumptions regarding features of the distributions of the effect sizes and estimation error, its performance may be sensitive to violations of these assumptions. To reduce the risk of extreme violations, when we apply MTAG, we impose three additional SNP filters beyond the standard filters used in a GWAS.

First, we restrict the set of SNPs to those with a minor allele frequency greater than 1%. This filter is motivated by the homogeneous Ω assumption and by the assumption that each SNP explains the same amount of phenotypic variation in expectation. Rare variants may follow a different effect size distribution both in terms of the variance and covariance of their effect sizes, which could bias the MTAG estimates.

Second, for each trait, we restrict variation in SNP sample sizes by calculating the 90th percentile of the SNP sample size distribution and removing SNPs with a sample size smaller than 75% of this value. This filter is similar to, although slightly more strict than, the sample size filter recommended for LD score regression¹⁴. If a SNP's effect is estimated in a relatively small subset of the sample, then the sample overlap across traits will likely be different for that SNP than for other SNPs in the sample. In that case, the covariance of the estimation error across traits as estimated by LD score regression may not be a good approximation to the covariance of the estimation error for that particular SNP.

Third, we drop SNPs in genomic regions containing SNPs that are outliers with respect to their effect size estimates. Because the effect sizes of these SNPs appear to have a different variance-covariance matrix than the rest of the genome, including these regions would likely lead to the biases and inefficiencies that can occur when the homogeneous Ω assumption is violated. In our empirical application, in the GWAS of NEUR, the effect sizes of SNPs in a region of chromosome 8 that tag an inversion polymorphism have been found to be strongly inflated relative to the effects estimated for SNPs in all other regions of the genome^{10,11}. Therefore, we omit SNPs in chromosome 8 between base-pair positions 7,962,590 and 11,962,591 (Supplementary Table 10).

GWAS-equivalent sample size for MTAG. The increase in the mean χ^2 statistic for each trait from the GWAS results to the MTAG results can be used to calculate a 'GWAS-equivalent sample size' for MTAG. Under the assumptions of LD score regression¹⁴, the expected χ^2 statistic for some SNP with LD score ℓ_j is

$$E(\chi_j^2 | \ell_j) = \frac{N_j h^2 \ell_j}{M} + N_j a + 1$$

where N_j is the sample size for SNP j , h^2 is the SNP heritability of the trait; M is the number of SNPs for which we define the SNP heritability, and a is the variance due to biases (for example, due to population stratification). Note that $E(\chi_j^2 | \ell_j) - 1$ scales linearly with N_j as long as M and ℓ_j are held constant in the additional samples^{24–26}. Because the individuals included in all GWAS are of European ancestry, M and ℓ_j are indeed expected to be approximately constant^{24–26}. Thus, we can use the mean χ^2 statistic from the GWAS and the MTAG results to calculate how much larger the GWAS sample size would have to be to give a mean χ^2 statistic equal to that attained by MTAG

$$N_{\text{GWAS-equiv},j} = N_{\text{GWAS},j} \frac{\overline{\chi_{\text{MTAG}}^2} - 1}{\overline{\chi_{\text{GWAS}}^2} - 1}$$

where $\overline{\chi_{\text{GWAS}}^2}$ is the mean χ^2 statistic in the GWAS results and $\overline{\chi_{\text{MTAG}}^2}$ is the mean χ^2 statistic in the MTAG results. Put another way, conducting MTAG gives the same power (as measured by mean χ^2 statistic) as conducting GWAS in a sample size that is larger by a factor of $\frac{\overline{\chi_{\text{MTAG}}^2} - 1}{\overline{\chi_{\text{GWAS}}^2} - 1}$. For DEP, going from GWAS to MTAG, the

mean χ^2 statistic increased from 1.44 to 1.60, implying an increase in the GWAS-equivalent sample size by a factor of

$$\frac{1.550 - 1}{1.434 - 1} = 1.26$$

Thus, the MTAG analysis has statistical power equivalent to a GWAS of DEP conducted in $354,861 \times 1.26\% = 449,649$ individuals. For NEUR, the mean χ^2 statistic rose from 1.284 to 1.557, implying a GWAS-equivalent sample size for MTAG that is 96% larger than the GWAS sample size: the effective sample size is $168,105 \times 1.96\% = 329,835$ individuals. For SWB, the mean χ^2 statistics rose from 1.308 to 1.570, implying a GWAS-equivalent sample size 85% larger than the GWAS: $388,538 \times 1.85\% = 718,284$ individuals (Supplementary Table 11).

MTAG results. The estimated matrices $\widehat{\Omega}$ and $\widehat{\Sigma}_{LD}$ (the LD score regression intercepts) are found in Supplementary Tables 12 and 13, respectively. Quantile–quantile plots corresponding to both the GWAS and MTAG results show an increase in power for each trait (Supplementary Fig. 7). Lead SNPs with a P value less than 1×10^{-5} from the MTAG analysis for each trait are listed in Supplementary Table 14.

Replication results. To test for sample overlap, we estimated the bivariate LD score regression intercept between the GWAS summary statistics for each discovery and each replication sample (Supplementary Table 15). The replication results are in Fig. 5 and Supplementary Table 16.

Polygenic prediction. We used the HRS²⁷ and Add Health as our prediction cohorts. We applied the same SNP filters as in the main MTAG analyses. Additionally, we restricted the set of SNPs used to construct the scores to HapMap3 SNPs for comparability across the two prediction cohorts. We calculated the SNP weights using the software package LDpred, assuming a fraction of causal SNPs equal to 1. The scores were constructed in PLINK using genotype probabilities obtained from 1000 Genomes imputation.

Bootstrapped confidence intervals were calculated by drawing, with replacement, a sample of equal size to the prediction sample and then calculating the incremental R^2 for the GWAS-based polygenic score, the MTAG-based polygenic score, and the difference between them. Our pooled results were obtained as a sample-size-weighted sum of HRS and Add Health results. As the bounds of the 95% confidence intervals, we used the 2.5th and 97.5th percentile values of the incremental R^2 across 1,000 bootstrap draws. Incremental R^2 estimates and their confidence intervals for the prediction analyses are in Supplementary Tables 17–20 and Supplementary Fig. 8.

Expected increase in polygenic score predictive power from MTAG. The phenotypic value of a trait in individual i , denoted y_i , can be decomposed into the sum of the additive genetic variance component and a residual

$$y_i = g_i + \varepsilon_i^y$$

We denote the GWAS- and MTAG-based polygenic scores for the trait by $\widehat{g}_{\text{GWAS},i}$ and $\widehat{g}_{\text{MTAG},i}$, respectively. Note that GWAS and MTAG produce consistent estimates of the SNP effect sizes, and LDpred²² produces a consistent estimate

of the additive genetic variance component. Therefore, each polygenic score $k \in \{\text{GWAS}, \text{MTAG}\}$ is approximately equal to g_i plus estimation error

$$\widehat{g}_{k,i} = g_i + \varepsilon_{k,i}$$

By the central limit theorem, the estimation error is approximately normally distributed

$$\varepsilon_{k,i} \sim N(0, V_k)$$

The variance V_k is inversely proportional to the sample size as long as the effective number of chromosome segments, M_p , is the same in every GWAS sample in the analysis^{24–26}. As in the calculation of the GWAS-equivalent sample size, where we assume that M_e is the same in every GWAS sample and in the prediction sample, the expected predictive power of a polygenic score is

$$E(R_k^2) = \frac{(h^2)^2}{h^2 + V_k}$$

where h^2 is the SNP heritability of the trait^{28–30}. (Note that if M_e were to differ greatly across samples, then it would be important to take this into account when calculating the expected predictive power^{24,25}.)

Using the GWAS results, we obtain an estimate of h^2 using LD score regression¹⁴ and an estimate of $E(R_k^2)$ from the predictive power of the GWAS-based polygenic score. Plugging these estimates into the above formula, we solve for an estimate of V_{GWAS} . We then multiply this value by $\frac{\overline{\chi_{\text{GWAS}}^2} - 1}{\overline{\chi_{\text{MTAG}}^2} - 1}$, which

we showed previously is equal to the ratio of the GWAS sample size to MTAG's GWAS-equivalent sample size, to obtain an estimate of V_{MTAG} . Substituting this back into the above formula along with our estimate of h^2 gives us the expected predictive power of the MTAG-based polygenic score.

Results of this calculation are found in Supplementary Table 17c. For DEP, NEUR, and SWB, respectively, we anticipated increases in predictive power of 0.21, 0.56, and 0.39 percentage points. All three anticipated increases were within their respective estimated confidence intervals: [0.04, 0.31], [0.16, 0.61], and [0.12, 0.65]. Overall, the observed gains in predictive power relative to conventional GWAS-based polygenic scores are thus consistent with theoretical expectations.

Biological annotation. Detailed results from DEPICT for each trait are found in Supplementary Tables 21–29. The GWAS- and MTAG-based tissue enrichment estimates for DEP, NEUR, and SWB are compared in Fig. 7 and Supplementary Figs. 9 and 10, respectively. The complete set of results from DEPICT is summarized in Supplementary Table 30.

Comparative analyses. We conducted analyses comparing MTAG to other multi-trait methods that can be applied in the specific setting for which MTAG was developed (Supplementary Note, Supplementary Figs. 11–13 and Supplementary Table 31).

Data availability. Summary statistics can be found at <http://www.thessgac.org/data>. For analyses that include data from 23andMe, only up to 10,000 SNPs can be reported. The GWAS of NEUR does not include data from 23andMe, so full summary statistics are available. For the GWAS of DEP and SWB and for the MTAG of NEUR and SWB, clumped results for SNPs with $P < 1 \times 10^{-5}$ are provided. For the MTAG of DEP, clumped results for SNPs with $P \leq 6.68 \times 10^{-3}$ are provided; this P -value threshold was chosen such that the total number of SNPs across the analyses that include data from 23andMe is equal to 10,000.

URLs. MTAG software is available at <https://github.com/omeed-maghzian/mtag/>. Social Science Genetic Association Consortium (SSGAC) website, <https://www.thessgac.org/data>.

Life Sciences Reporting Summary. Further information on experimental design is available in the Life Sciences Reporting Summary.

Code availability. MTAG software is available at <https://github.com/omeed-maghzian/mtag/>.

References

- Vilhjálmsdóttir, B. J. et al. Modeling linkage disequilibrium increases accuracy of polygenic risk scores. *Am. J. Hum. Genet.* **97**, 576–592 (2015).
- Yang, J. et al. Genomic inflation factors under polygenic inheritance. *Eur. J. Hum. Genet.* **19**, 807–812 (2011).
- Wientjes, Y. C. J., Bijma, P., Veerkamp, R. F. & Calus, M. P. L. An equation to predict the accuracy of genomic values by combining data from multiple traits, populations, or environments. *Genetics* **202**, 799–823 (2016).

25. Lee, S.H., Clark, S. & van der Werf, J. Estimation of genomic prediction accuracy from reference populations with varying degrees of relationship. Preprint at *bioRxiv* <https://doi.org/10.1101/119164> (2017).
26. Lee, S. H., Weerasinghe, W. M. S. P., Wray, N. R., Goddard, M. E. & van der Werf, J. H. J. Using information of relatives in genomic prediction to apply effective stratified medicine. *Sci. Rep.* **7**, 42091 (2017).
27. Sonnega, A. et al. Cohort profile: the Health and Retirement Study (HRS). *Int. J. Epidemiol.* **43**, 576–585 (2014).
28. Daetwyler, H. D., Villanueva, B. & Woolliams, J. A. Accuracy of predicting the genetic risk of disease using a genome-wide approach. *PLoS One* **3**, e3395 (2008).
29. Wray, N. R. et al. Pitfalls of predicting complex traits from SNPs. *Nat. Rev. Genet.* **14**, 507–515 (2013).
30. Pasaniuc, B. & Price, A. L. Dissecting the genetics of complex traits using summary association statistics. *Nat. Rev. Genet.* **18**, 117–127 (2017).

Life Sciences Reporting Summary

Nature Research wishes to improve the reproducibility of the work we publish. This form is published with all life science papers and is intended to promote consistency and transparency in reporting. All life sciences submissions use this form; while some list items might not apply to an individual manuscript, all fields must be completed for clarity.

For further information on the points included in this form, see [Reporting Life Sciences Research](#). For further information on Nature Research policies, including our [data availability policy](#), see [Authors & Referees](#) and the [Editorial Policy Checklist](#).

▶ Experimental design

1. Sample size

Describe how sample size was determined.

For each of the three phenotypes, we combined all publicly available summary statistics with summary statistics from new association analyses. Details are reported in Section 3.2 of the Supplementary Note.

2. Data exclusions

Describe any data exclusions.

No data were excluded from the analysis (except for standard quality-control filters applied to the SNP data, described in Supplementary Note sections 3.2 and 3.3 and Supplementary Table 10).

3. Replication

Describe whether the experimental findings were reliably reproduced.

We test the MTAG-identified lead SNPs jointly for replication. Their replication record is strong; see Figure 5 and Supplementary Note section 5.

4. Randomization

Describe how samples/organisms/participants were allocated into experimental groups.

Not relevant because the study is not experimental.

5. Blinding

Describe whether the investigators were blinded to group allocation during data collection and/or analysis.

Not relevant because the study is not experimental.

Note: all studies involving animals and/or human research participants must disclose whether blinding and randomization were used.

6. Statistical parameters

For all figures and tables that use statistical methods, confirm that the following items are present in relevant figure legends (or the Methods section if additional space is needed).

- | | |
|-------------------------------------|--|
| n/a | Confirmed |
| <input type="checkbox"/> | <input checked="" type="checkbox"/> The <u>exact</u> sample size (n) for each experimental group/condition, given as a discrete number and unit of measurement (animals, litters, cultures, etc.) |
| <input type="checkbox"/> | <input checked="" type="checkbox"/> A description of how samples were collected, noting whether measurements were taken from distinct samples or whether the same sample was measured repeatedly. |
| <input checked="" type="checkbox"/> | <input type="checkbox"/> A statement indicating how many times each experiment was replicated |
| <input type="checkbox"/> | <input checked="" type="checkbox"/> The statistical test(s) used and whether they are one- or two-sided (note: only common tests should be described solely by name; more complex techniques should be described in the Methods section) |
| <input type="checkbox"/> | <input checked="" type="checkbox"/> A description of any assumptions or corrections, such as an adjustment for multiple comparisons |
| <input type="checkbox"/> | <input checked="" type="checkbox"/> The test results (e.g. p values) given as exact values whenever possible and with confidence intervals noted |
| <input type="checkbox"/> | <input checked="" type="checkbox"/> A summary of the descriptive statistics, including central tendency (e.g. median, mean) and variation (e.g. standard deviation, interquartile range) |
| <input type="checkbox"/> | <input checked="" type="checkbox"/> Clearly defined error bars |

See the web collection on [statistics for biologists](#) for further resources and guidance.

► Software

Policy information about [availability of computer code](#)

7. Software

Describe the software used to analyze the data in this study.

The GWASs in the UKB and replication cohorts were done with SNPtest v2.5.2. Meta-analyses were performed with Metal, release 2011-03-25. QC was run with EasyQC v9.0. Simulated results were generated and replication analyses were conducted using Python v2.7. LD score regressions were done using ldsc v1.0.0. Clumping was performed with Plink, 1.90b3p. Polygenic score weights were generated using LDpred v0.9.09 and the prediction analyses were executed in Stata v14.2. Biological annotation was completed using DEPICT (downloaded Feb 2015). The comparative analyses estimates for Shom and Shet were calculated using the R package CPASSOC v1.01. MTAG analyses were conducted in Python v2.7.

For all studies, we encourage code deposition in a community repository (e.g. GitHub). Authors must make computer code available to editors and reviewers upon request. The *Nature Methods* [guidance for providing algorithms and software for publication](#) may be useful for any submission.

► Materials and reagents

Policy information about [availability of materials](#)

8. Materials availability

Indicate whether there are restrictions on availability of unique materials or if these materials are only available for distribution by a for-profit company.

No unique materials were used.

9. Antibodies

Describe the antibodies used and how they were validated for use in the system under study (i.e. assay and species).

No antibodies were used.

10. Eukaryotic cell lines

a. State the source of each eukaryotic cell line used.

No eukaryotic cell lines were used.

b. Describe the method of cell line authentication used.

No eukaryotic cell lines were used.

c. Report whether the cell lines were tested for mycoplasma contamination.

No eukaryotic cell lines were used.

d. If any of the cell lines used in the paper are listed in the database of commonly misidentified cell lines maintained by [ICLAC](#), provide a scientific rationale for their use.

No cell lines were used.

► Animals and human research participants

Policy information about [studies involving animals](#); when reporting animal research, follow the [ARRIVE guidelines](#)

11. Description of research animals

Provide details on animals and/or animal-derived materials used in the study.

No animals were used.

Policy information about [studies involving human research participants](#)

12. Description of human research participants

Describe the covariate-relevant population characteristics of the human research participants.

Analyses were conducted on GWAS summary statistics. References to the studies that report covariate-relevant population characteristics are in Supplementary Table 2 and Supplementary Note section 3.2.